

68
21
55
3

**SOME CONSIDERATIONS OF
WIDE APERTURE LOCALIZER ANTENNAS**

By
Chester B. Watts, Jr
Electronics Division

Technical Development Report No 155



**CIVIL AERONAUTICS ADMINISTRATION
TECHNICAL DEVELOPMENT AND
EVALUATION CENTER
INDIANAPOLIS, INDIANA**

January 1952

1400

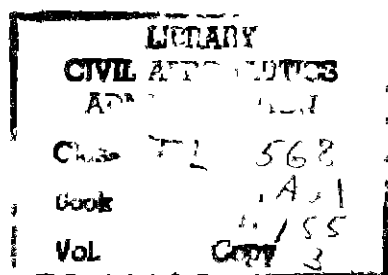
U S DEPARTMENT OF COMMERCE

Charles Sawyer, Secretary

CIVIL AERONAUTICS ADMINISTRATION

C F Horne, Administrator

D M Stuart, Director, Technical Development and Evaluation Center



L 111
This is a technical information report and does not
necessarily represent CAA policy in all respects

TABLE OF CONTENTS

	Page
SUMMARY	1
THE PROBLEM	1
DEFINITION OF TERMS	1
ARRAY TYPE A	3
ARRAY TYPE B	6
PHYSICAL DESIGN	8
CONCLUSIONS	10

Manuscript received April 1951

SOME CONSIDERATIONS OF WIDE APERTURE LOCALIZER ANTENNAS

SUMMARY

The development of two possible types of wide aperture localizer antennas is outlined, both of which are based on the use of waveguide-fed slot elements. It is concluded that the methods described have promise and should receive experimental investigation.

THE PROBLEM

As with other radio navigation facilities, the nature of the site has considerable effect upon the performance of an instrument landing localizer. One way in which improved performance at any given site can be secured is through control of the azimuth directivity of the localizer antenna patterns, it being generally true that the more the radiated energy can be confined to a narrow sector lying down the runway, the less will be the influence of the site.

The problem under consideration is the development of means for confining the energy to a sector, the width of which is to be based on factors other than antenna complexity. There seem to be, principally, two such factors. The first has to do with the angular width of linear course deviation indicator current. The second has to do with the distance from the array at which the patterns become resolved. At the present frequency of 110 Mc, the second factor would appear to be the limiting one as regards the pattern sharpness.

At a given point of observation, the phase error, due to proximity, between the ends and middle of a broadside array is closely given by the formula

$$e = \frac{A^2 \cos^2 \theta}{8D} \quad (1)$$

in which the error e is expressed as a path length, A is the total aperture of the array, D is the distance between the array and the observer, and θ is the azimuth of the observer with respect to the array, measured from the normal. Thus, for example, if one decides to tolerate a maximum value for phase error of 30° , which at 110 Mc corresponds to a path length of about three-fourths foot, while the aperture A is, say, 200 feet, then the value for D as given by equation (1) is 6,700 feet for an observer straight ahead. Fig. 1 illustrates the situation. Here are plotted the curves which

are loci of constant phase error e equal to 30° for various apertures.

With full utilization of a 200-foot aperture, then, while it can be shown that good indicator linearity is still obtainable, the matter of proximity phase error begins to become a problem. This difficulty would be reduced by an increase in carrier frequency.

It should be noted, before leaving the subject of proximity phase error, that some compensation for the effect is possible. As an example, if the 200-foot linear array were bent into a circular arc of radius 6,700 feet, then there would be no phase error at 6,700 feet, while the tolerable 30° error would exist at infinity and again at 3,300 feet in front of the array.

Having once established a maximum aperture which can be allowed from a standpoint of proximity phase error, the problem which now remains is the design of an array which will fully utilize this aperture.

DEFINITION OF TERMS

The radiation from any localizer may be considered as being divided into two parts, each part having its own amplitude and phase distributions in azimuth, and each part serving its own particular purpose in the receiver.

The first part will be called the deflection component and is known otherwise by the names sideband and cloverleaf signal. It may be radiated with an azimuth distribution as indicated by curve A, Fig. 2. The pattern is usually essentially constant phase, except that the part below the axis indicates complete 180° phase reversal. In the receiver the deflection component serves the purpose of deflecting the course deviation indicator. The course is defined as the locus of points having no indicator deflection, hence, zero deflection component. Reflections of deflection component from objects near the localizer site, which result in a value other than zero for the deflection component along the runway centerline extension cause course bends.

The second part will be called the reference component and is known otherwise by the names carrier and dumbbell signal. It may be radiated with an azimuth distribution as indicated by curve B, Fig. 2. The pattern is usually essentially constant phase, or if not, should track in phase with the deflection component, except that there is no 180° phase reversal. In the receiver, the reference

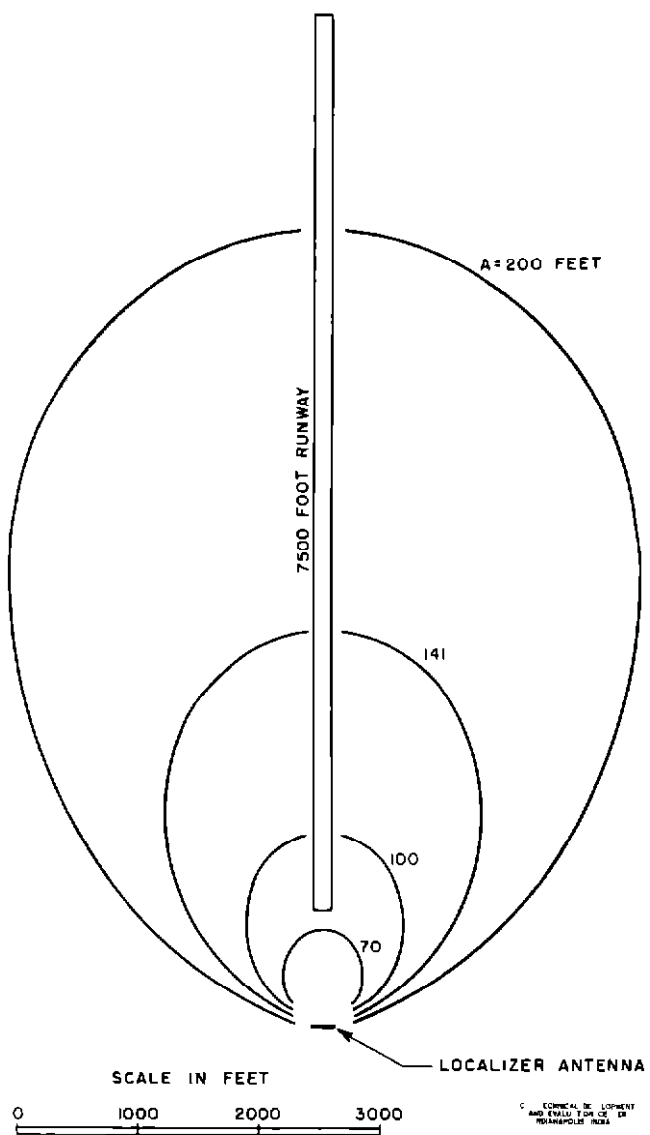


Fig 1 Loci of Constant Phase Error of 30 Degrees for Various Values of Aperture A at 110 Megacycles

component serves the purpose of providing an amplitude and phase standard, against which the deflection component is compared. In the absence of deflection component, the deviation indicator is not deflected by reference component in any amplitude or phase. Site reflections of reference component do not produce course bends.

The reference and deflection components must be characterized by different types of modulation so that, in the receiver, each may be separated and treated according to its own purpose.

In the case of a tone localizer, the reference component may be a signal of the

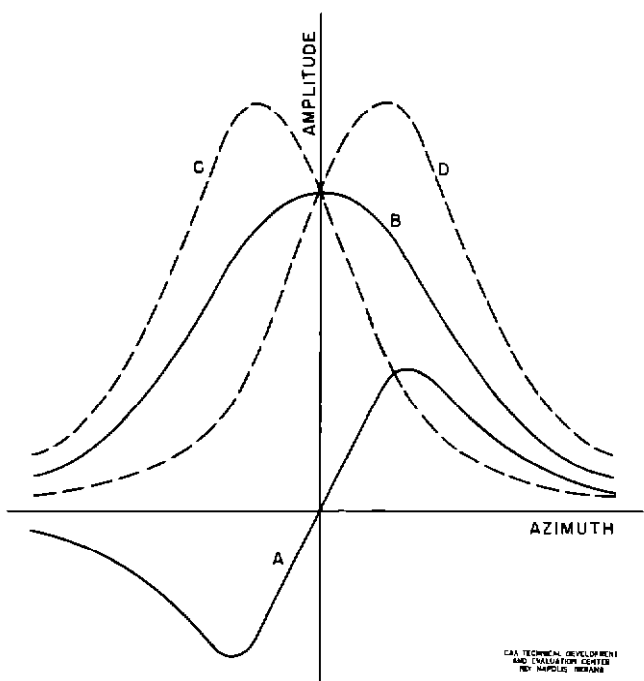


Fig 2 Component Field Patterns

form

$$E_r = A_r [1 + m (\sin \alpha_1 t + \sin \alpha_2 t)] \sin \omega t \quad (2)$$

while the deflection component may be a signal of the form

$$E_d = A_d (\sin \alpha_1 t - \sin \alpha_2 t) \sin \omega t \quad (3)$$

Since this arrangement results in the production of sidebands of α_1 and α_2 frequency in both the reference and the deflection components, it is a common practice to consider the azimuth distribution of the total sideband components, shown plotted as the dotted curves labeled C and D in Fig 2. This practice, however, can lead to confusion when the total sideband patterns are used to analyze localizer performance. It should be remembered that it is pattern A, which is the difference of patterns C and D, which represents the desired distribution of deflection component signal. It is this signal which accounts for all departures of the course deviation indicator from center, whether this signal reaches the receiver via the direct route or via site reflections, whether horizontally or vertically polarized, whether radiated by the antenna array or as leakage from the transmitter.

Since it is clearly the site reflection of deflection component which causes course bends, the basis of comparing the bend reducing effectiveness of two localizers should

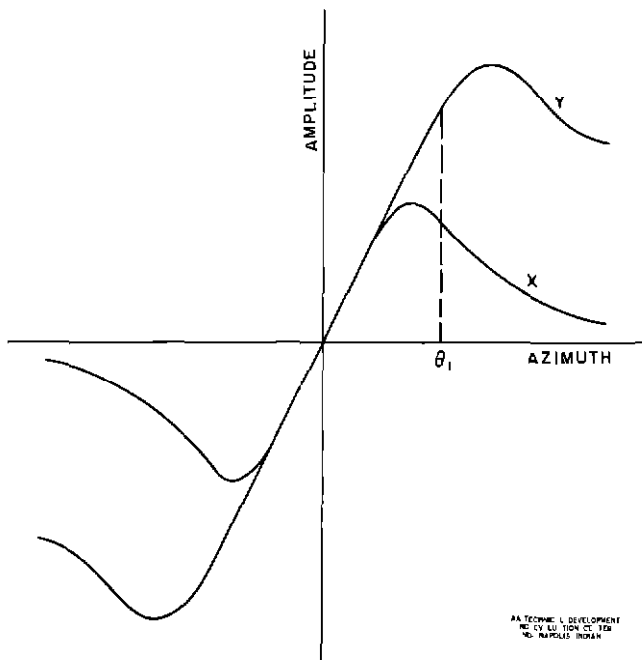


Fig. 3 Comparison of Deflection Component Field Patterns

be their deflection component patterns. Fig. 3 shows deflection component field patterns of two hypothetical localizers X and Y. The patterns are plotted with the same initial slope. This means that when paired with a suitable reference component, either pattern would produce a course of the same width or sensitivity. Now consider a site reflector which has a bearing angle θ_1 with respect to the antenna array. The ratio of the ordinates of the two curves X and Y at the angle θ_1 should be equal to the ratio of the course bend amplitudes which would be produced by the reflector in either case. This ratio is named bend reduction factor, R, and, for

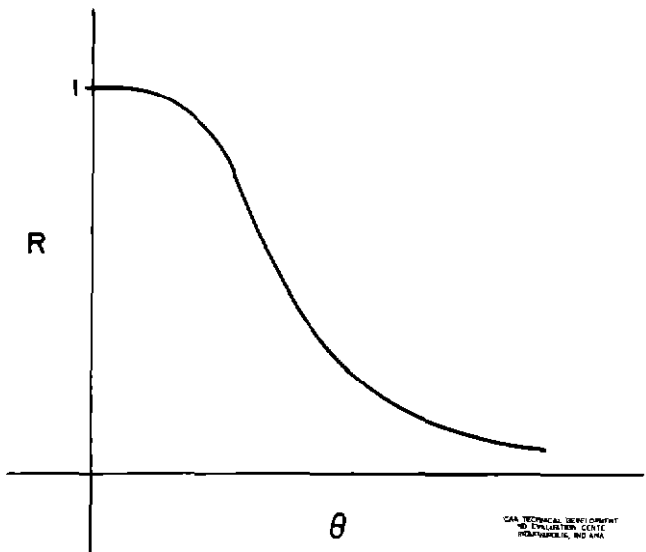


Fig. 4 Bend Reduction Factor for Pattern X Versus Pattern Y

the two hypothetical localizers, has the form shown in Fig. 4. The value of R will always be unity at zero azimuth angle, but for high relative effectiveness should rapidly decrease to a low value with increasing azimuth angle and should remain low.

ARRAY TYPE A

Consider a symmetrical linear array as in Fig. 5 having a single central element plus symmetrical pairs of elements. The spacing between adjacent elements is a constant S . If p is the number of a particular element, counting from the center, the element current is I_p on the right and I_{-p} on the left. Suppose the feed system is such that it can be represented by an equivalent circuit

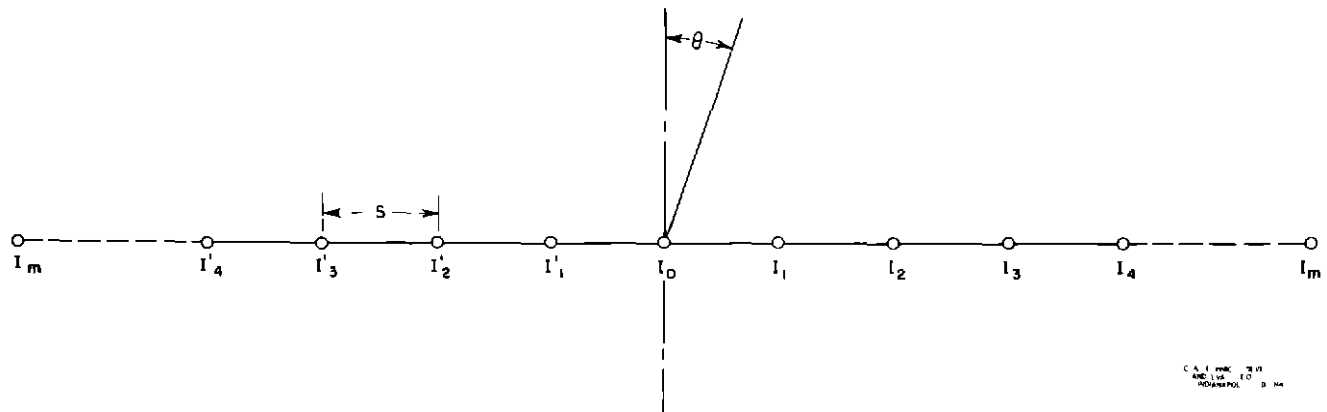


Fig. 5 Linear Array

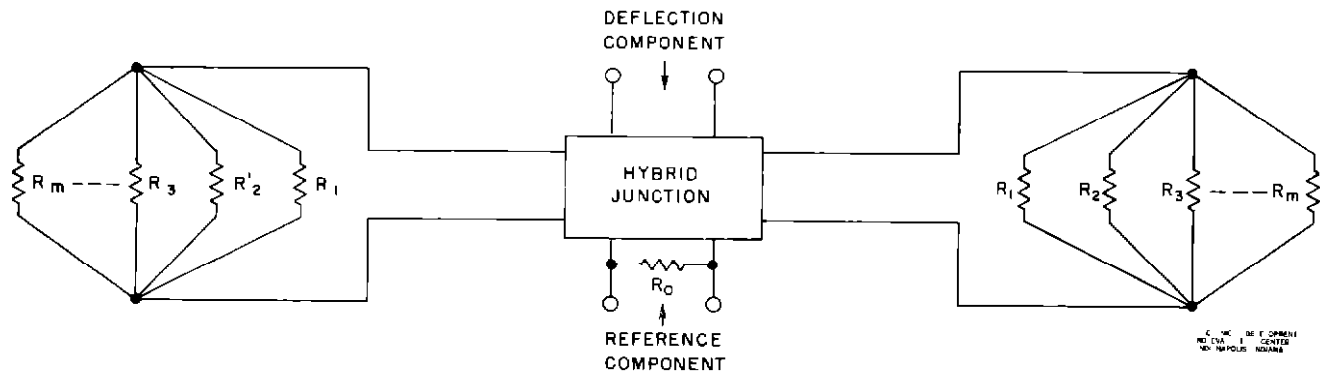


Fig. 6 Equivalent Circuit, Array Type A

as in Fig. 6. The current distribution $I(p)$ is controlled by regulating the value of each element's shunt impedance R .

An array of this type may have a considerable advantage over the present conventional types as regards the simplicity of extension to large apertures. However, it also has an important limitation, in that the current distributions for deflection component and for reference component are not mutually independent. This means that if a current distribution is chosen which optimizes one pattern, then the shape of the other pattern is determined, and must be either accepted or the whole arrangement rejected.

Because of the importance of the deflection component field pattern in relation to site reflections, it is natural that this pattern be chosen as the one to be optimized. Having done this, it will be of interest to see what results in the way of reference component pattern.

Let us consider first the production of a deflection component pattern which rises to a maximum at an angle of 5° from the course, then drops rapidly to a very low level, and has no minor lobes of appreciable magnitude. This will be a pattern having about twice the sharpness, and requiring about twice the aperture, of a standard 8-loop localizer.

It is well known that a current distribution in accordance with the coefficients of the binomial expansion $(a + b)^{n-1}$ results in a single-lobed pattern having, theoretically, no minor lobes whatever, provided the element spacing S is 180° or less. The field pattern is given by the equation

$$F(\theta) = z^{n-1} \cos^{n-1} \left(\frac{S}{2} \sin \theta \right) \quad (4)$$

in which n is the total number of elements. Also it is true that if a series is formed in which each term is the difference of successive binomial expansion coefficients, then a current distribution in accordance with such a series will produce a double-lobed pattern, free of minor lobes. The field pattern is given by the equation

$$F(\theta) = 2^{n-1} \sin\left(\frac{S}{2}\sin\theta\right) \cos^{n-2}\left(\frac{S}{2}\sin\theta\right) \quad (5)$$

The formation of the difference series may be illustrated by the following example

$$\begin{array}{cccccccccc}
 1 & 9 & 36 & 84 & 126 & 126 & 84 & 36 & 9 & 1 \\
 -1 & -9 & -36 & -84 & -126 & -126 & -84 & -36 & -9 & -1 \\
 \hline
 1 & 8 & 27 & 48 & 42 & 0 & -42 & -48 & -27 & -8 & -1
 \end{array}$$

Assuming the afore-mentioned type series is to be used as the basis for the current distribution for the deflection component pattern, it becomes necessary to select the series which has the proper number of terms to give the pattern sharpness desired. This may be done by setting

$$\frac{dF(\theta)}{d\theta} = 0 \quad (6)$$

for θ equal to 5° , and solving for n , the total number of terms. Since the values of angle θ involved are rather small, this procedure can be simplified by the use of the small angle approximations for sine and cosine functions, and it is found that the necessary value for n is approximately 25, with an element spacing S equal to 254° . Substituting these values in equation (5) results in curve A, Fig. 7. The binomial difference series for n equal 25 may be tabulated, beginning at the center, as follows:

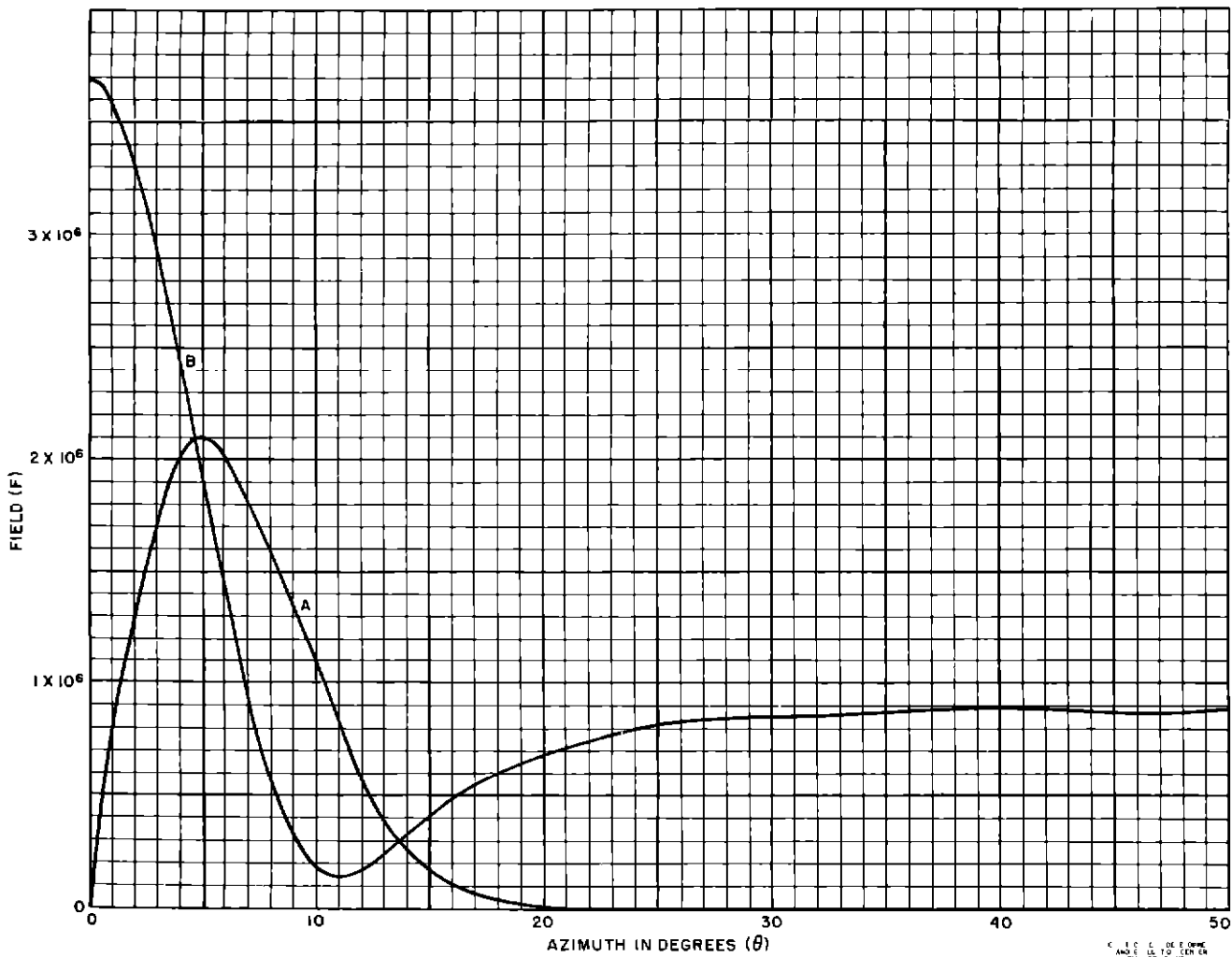


Fig 7 Component Field Patterns, 85-Foot Aperture, Array Type A

TABLE I

P	I_A	P	I_A
0	0	7	24,794
1	208,012	8	7,084
2	326,876	9	1,518
3	326,876	10	230
4	245,157	11	22
5	144,210	12	1
6	67,298		

It will be observed that several of the terms near the end are so small that their total contribution to the field pattern is negligible. In fact, it is found that, if the terms for p equal 8 through 12 are omitted, the minor lobes resulting are more than 40 db down from the maximum, and the resulting pattern does not differ by the width of the line from that given in curve A, Fig 7.

Thus the physical array may be considered as comprising seven pairs of elements, plus a center element which carries no deflection component current. This gives the array an aperture

$$A = 2mS = 3456^\circ \quad (7)$$

which corresponds to about 85 feet at 110 Mc. With the standard 8-loop localizer as a basis of comparison, the deflection component pattern, curve A, Fig 7, has a bend reduction factor R versus azimuth as shown plotted in Fig 8.

To obtain the reference component pattern, curve B, Fig 7, it is necessary to compute the summation of seven in-phase pairs with amplitudes as given in Table I. The amplitude of the central element, which contains only reference component, is the one free choice available. It is chosen here

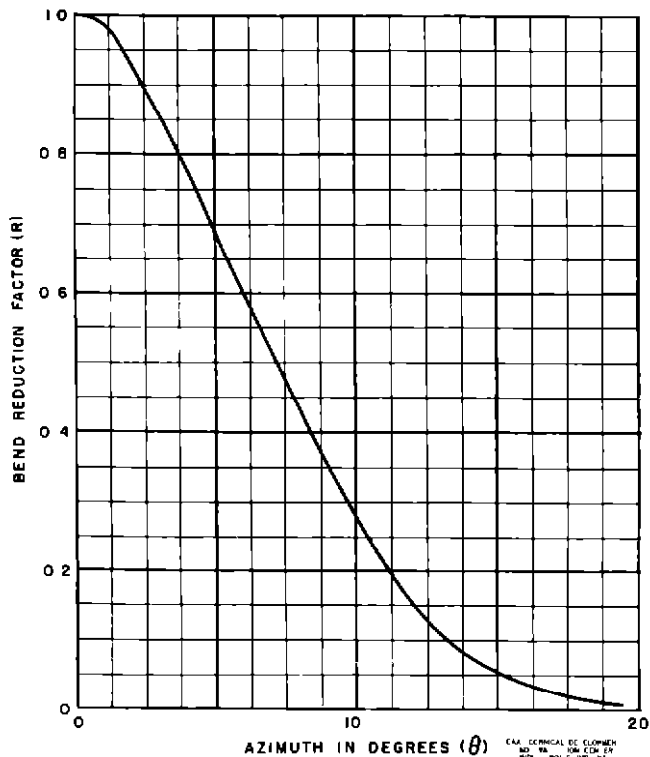


Fig. 8 Bend Reduction Factor for 85-Foot Aperture Array Versus Standard 8-Loop Array

so that the reference component pattern does not quite go negative at its lowest value

It is of interest to consider the deviation indicator current which would result with the patterns shown in Fig. 7. Within certain limits, deviation current is given closely by the relation

$$D = \frac{A}{B} \quad (8)$$

and is shown plotted for this case in Fig. 9. The limits mentioned are not particularly related to the antenna design, but have to do with modulation levels and the characteristics of the receiving system

ARRAY TYPE B

It would be desirable perhaps if the wide angle radiation of reference component in array Type A could be reduced without sacrificing the characteristics of the deflection component field pattern.

Consider again a symmetrical linear array as in Fig. 5, but having a feed system which may be represented by the equivalent circuit of Fig. 10. This arrangement is somewhat more difficult to deal with in theory, but not necessarily any more com-

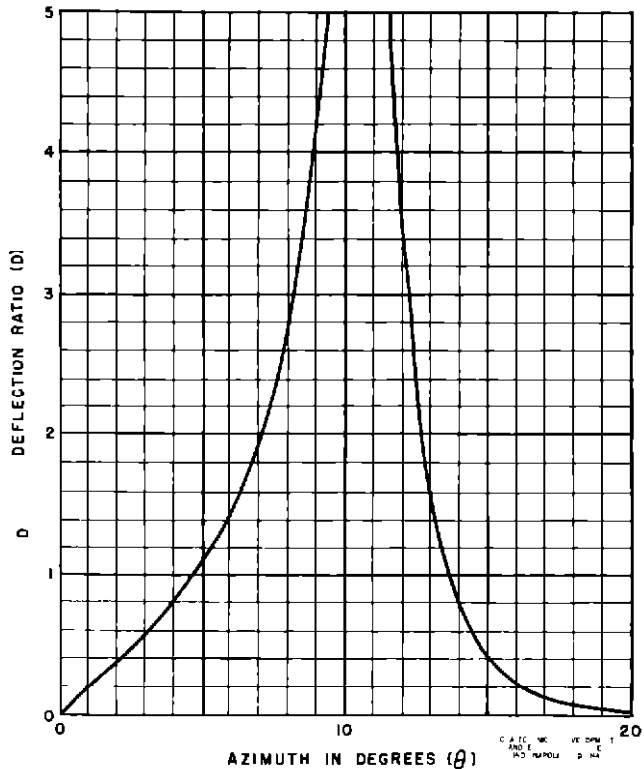


Fig. 9 Deflection Ratio for Component Patterns of Figure 7

plicated in practice than the Type A feed system

The resistances, which represent the shunt element impedances, are here connected not quite in parallel, but are separated each from the next by a delay device having a very small phase angle ϕ . Consider a wave passing down the line from left to right. The element current I_p in each case may be adjusted as before, by regulating the value of resistance R_p , but the phase of the current in each element will lag the current in the preceding element by approximately the angle ϕ if the energy taken by any one element is relatively small compared with the total. This means that the beam formed by the array is not normal to the line of the array, but lies at an angle θ_0 to the right of the normal, where

$$\theta_0 = \arcsin \frac{\phi}{S} \quad (9)$$

Similarly, in the case of a wave passing from right to left, the beam lies at an angle θ_0 to the left of the normal. If the reference component energy produces in-phase excitation of the right and left lobes, the deflection component energy will produce out-of-phase excitation of the same two lobes.

If the foregoing statements are true,

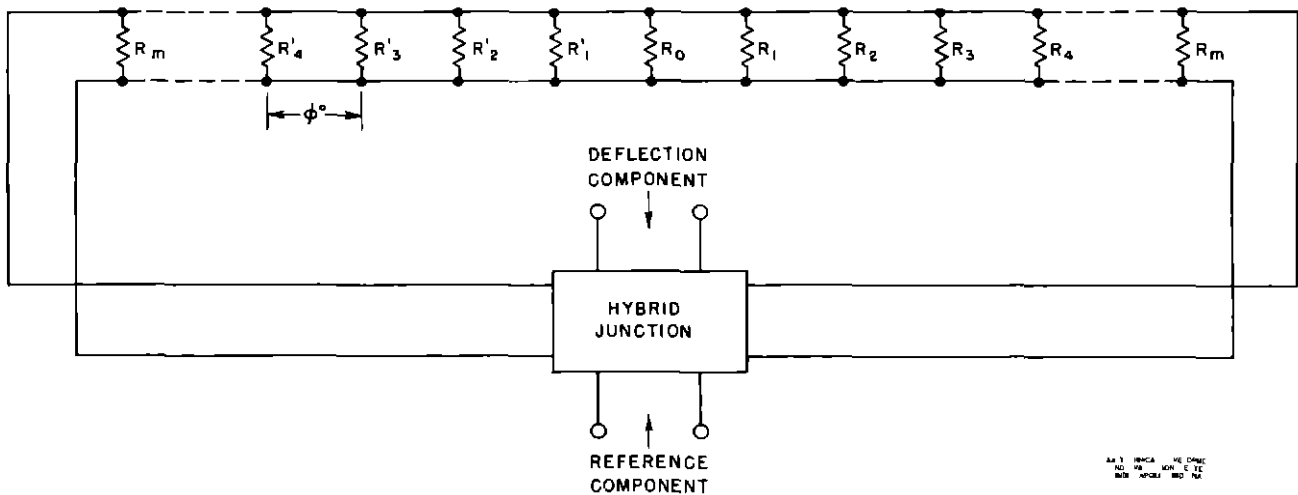


Fig 10 Equivalent Circuit, Array Type B

a new tool is available, for it can be shown that if the sum and difference are taken of two slightly displaced beams which are free of minor lobes, then the two new patterns which result may be free of minor lobes also.

Suppose the current distribution is such that the right and left beam patterns are of the binomial type so that

$$F_1(\theta) = 2^{n-1} \cos^{n-1} \left[\frac{S}{2} \sin(\theta - \theta_0) \right] \quad (10)$$

$$F_2(\theta) = z^{n-1} \cos^{n-1} \left[\frac{s}{z} \sin(\theta + \theta_0) \right] \quad (11)$$

These are shown plotted in Fig. 11 for values $n = 109$, $S = 254^\circ$ and $\theta_0 = 0.5^\circ$. The sum and difference patterns are shown in Fig. 12 as curve B and curve A respectively.

That the sum and difference patterns should be free of minor lobes may be shown as follows. The binomial distribution function for large values of n is found to be very

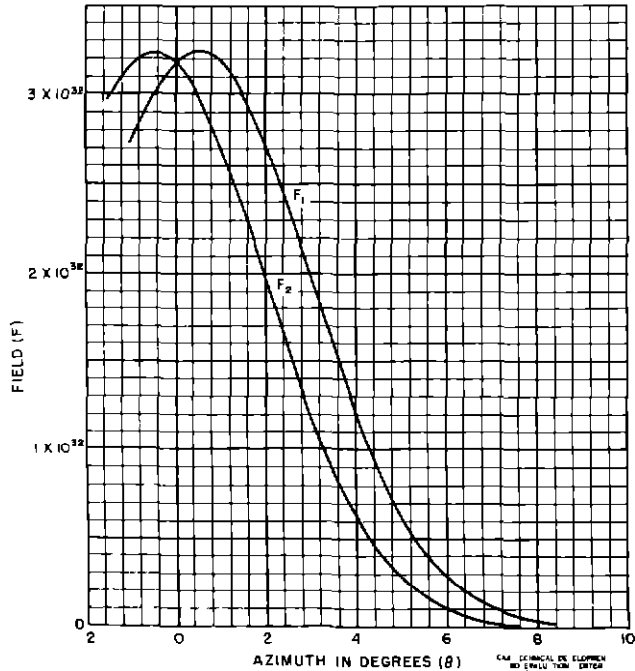


Fig. 11 Right and Left Beam Patterns, Array Type B

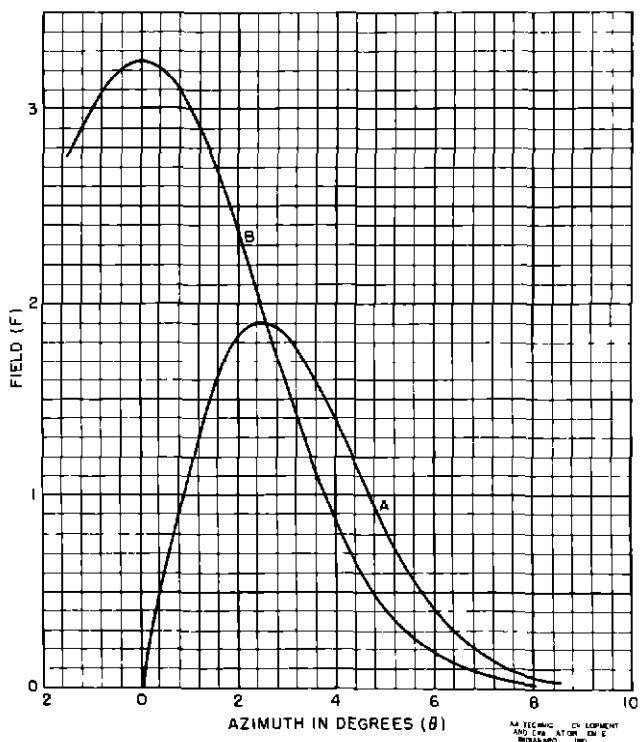


Fig 12 Component Field Patterns, 200-Foot Aperture, Array Type B

TABLE II

P	I_A	P	I_A	P	I_A	P	I_A
0	0	14	1.6971×10^{29}	28	3.5828×10^{24}	42	2.1690×10^{15}
1	4.5200×10^{29}	15	1.0542×10^{29}	29	1.1624×10^{24}	43	2.7471×10^{14}
2	8.5600×10^{29}	16	6.2647×10^{28}	30	3.5788×10^{23}	44	3.1552×10^{13}
3	1.1712×10^{30}	17	3.5625×10^{28}	31	1.0442×10^{23}	45	3.2595×10^{12}
4	1.3725×10^{30}	18	1.9384×10^{28}	32	2.8826×10^{22}	46	2.9987×10^{11}
5	1.4540×10^{30}	19	1.0090×10^{28}	33	7.5892×10^{21}	47	2.4268×10^{10}
6	1.4249×10^{30}	20	5.0237×10^{27}	34	1.7762×10^{21}	48	1.7013×10^9
7	1.3080×10^{30}	21	2.3869×10^{27}	35	4.2755×10^{20}	49	1.0115×10^8
8	1.1333×10^{30}	22	1.0921×10^{27}	36	9.2840×10^{19}	50	4.9621×10^6
9	9.3090×10^{29}	23	4.7260×10^{26}	37	1.8874×10^{19}	51	1.9281×10^5
10	7.2720×10^{29}	24	1.9599×10^{26}	38	3.5818×10^{18}	52	5.5640×10^3
11	5.4160×10^{29}	25	7.7533×10^{25}	39	6.3245×10^{17}	53	1.0600×10^2
12	3.8485×10^{29}	26	2.9228×10^{25}	40	1.0351×10^{17}	54	1.0000
13	2.6138×10^{29}	27	1.0493×10^{25}	41	1.5635×10^{16}		

closely approximated by the probability function

$$I_B = K_1 e^{-cp^2} \quad (12)$$

Similarly, the binomial difference series distribution is very closely approximated by the equation

$$I_A = K_2 p e^{-cp^2} \quad (13)$$

For a given aperture, the constant c has the same value for both equations. In this case c equals 0.0188. For arrays of relatively high sharpness, the antenna pattern is given by the Fourier transform of the current distribution. Furthermore, according to Campbell and Foster,¹ the Fourier transforms of both I_A and I_B are functions of exactly the same form. In other words, there exists here the interesting situation that the shapes of both field patterns are the same as the

shapes of the corresponding current distribution functions. In subtracting the right and left beam patterns, F_1 and F_2 , Fig. 11, which are identical except for a small displacement along the abscissa, the effect is to form the derivative, or to go from a function having the form of equation (12) to one having the form of equation (13). Both are free of minor lobes.

For reference, the current distribution I_A is given in Table II for $n = 109$. The values in the table were calculated, not by the approximation, but from the binomial difference series.

In the practical design of the physical array it should not be necessary to go much beyond p equal to 16 to achieve a sufficiently low level of minor lobes. This would correspond to an aperture of about 200 feet.

The bend reduction factor R and the deflection ratio D for these patterns are given in Figs. 13 and 14.

PHYSICAL DESIGN

The two arrays which have been described were planned with a specific physical arrangement in mind, viz., the combination

¹G. A. Campbell and R. M. Foster, "Fourier Integrals for Practical Applications," Bell Telephone Technical Publications, Monograph B-584, September 1931.

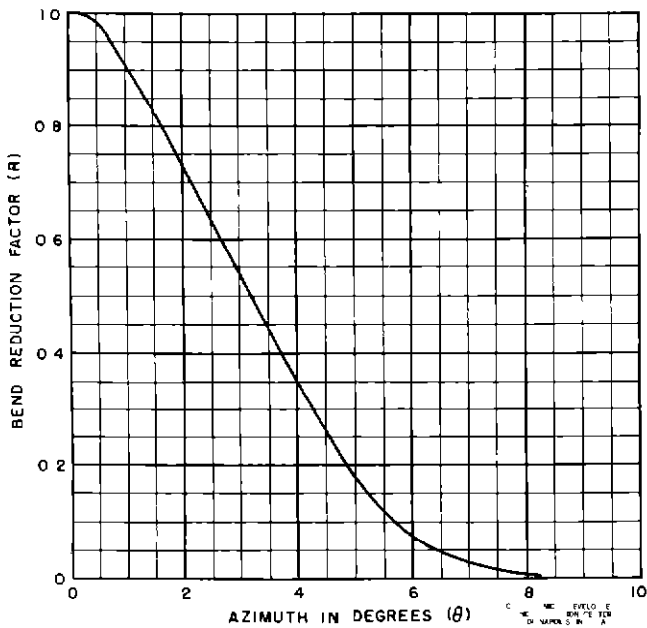


Fig. 13 Bend Reduction Factor for 200-Foot Aperture Array Versus Standard 8-Loop Array

of slot radiating elements with waveguide feed. However, there is no reason, other than considerations of complexity, why the slots could not be replaced by dipoles or loops, and the waveguide by transmission line.

Fig. 15 is intended to show the general nature of the Type A antenna. The drawing is neither to scale nor does the number of slots shown have any significance. The guide is excited in its dominant mode, with the electric field vertical. The two guide-feed probes, one a vertical whip, the other a half-loop, produce in-phase and out-of-phase excitation of the two halves of the guide. With

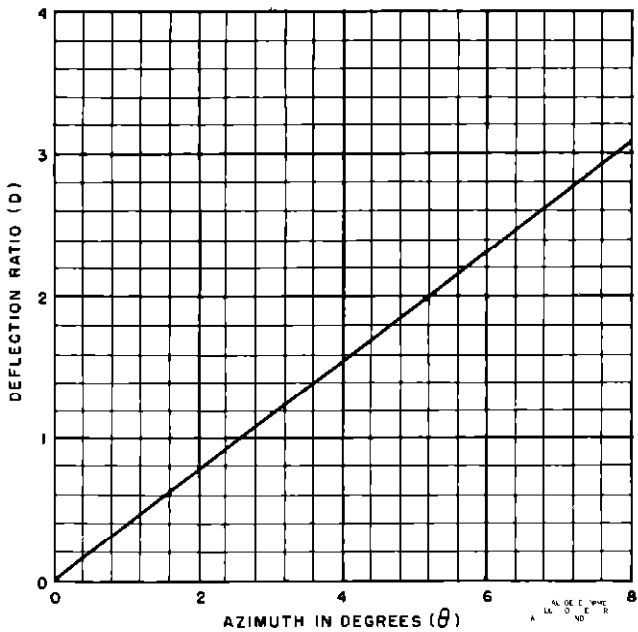


Fig. 14 Deflection Ratio for Component Patterns of Figure 12

the symmetrical disposition of the two feed probes, they do not couple one to the other, thus, they behave thoroughly as a hybrid junction. Each slot receives excitation by the guide through a hooked probe, not shown, which is mounted on the guide wall, immediately to one side of the slot. Orientation of the hook determines the polarity and magnitude of the slot current in each case.

The slots, in the case of the Type A antenna, are spaced $1/2$ guide wavelength apart, which puts them effectively in parallel as shown in the equivalent circuit, Fig. 6.

Fig. 16 represents the Type B Antenna. The construction would be quite similar, except for the location of the feed probes and

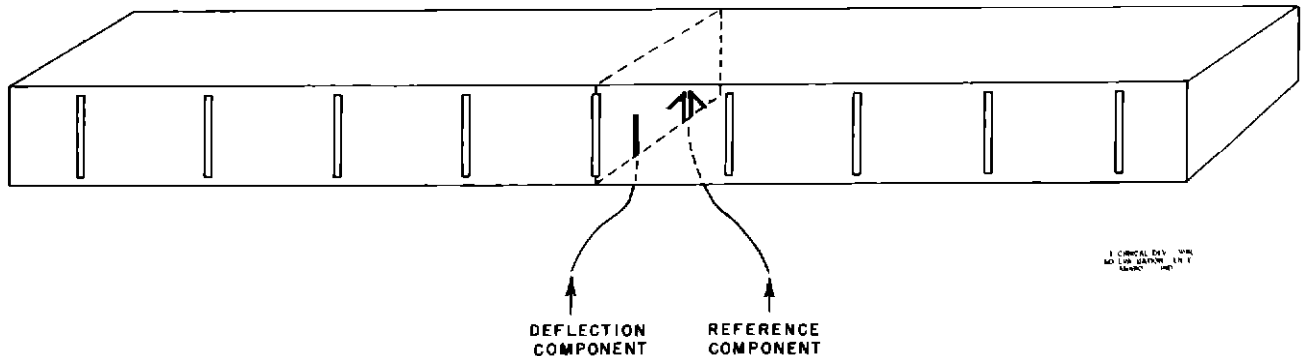


Fig. 15 Antenna Type A

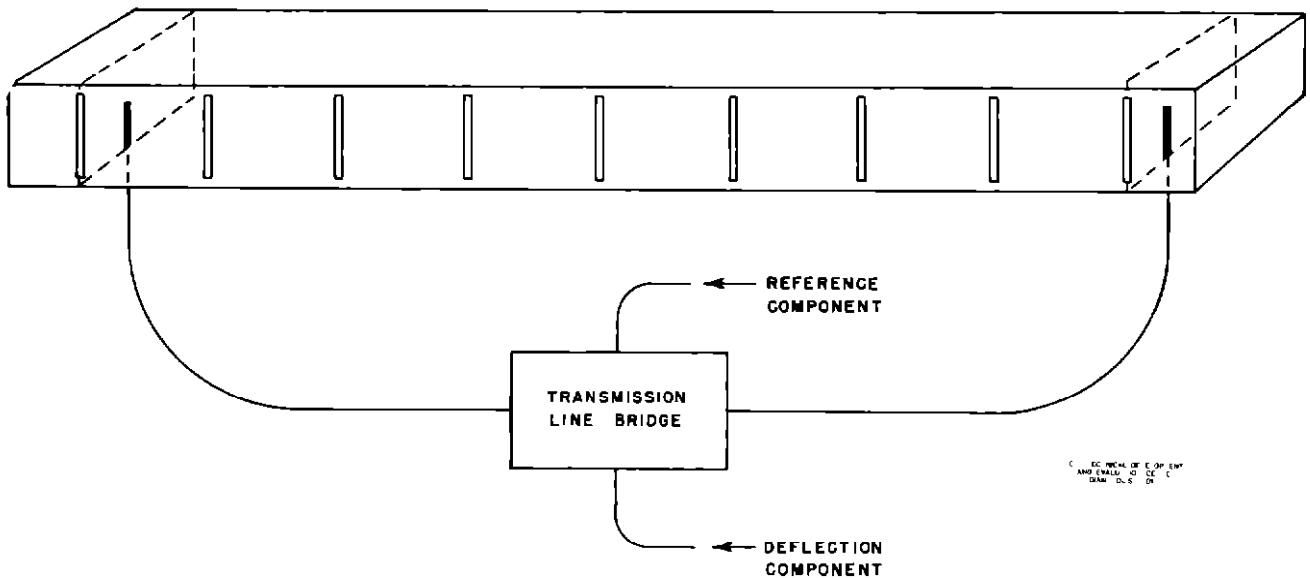


Fig 16 Antenna Type B

the fact that the slots are spaced slightly farther apart than $1/2$ guide wavelength. A transmission-line bridge external to the guide appears to be an effective means for obtaining the required guide excitation.

CONCLUSIONS

It is concluded that readily controllable localizer antenna arrays can be constructed, without undue complexity, to have almost any aperture that would be desired. The methods, which have been outlined, would bear further experimental investigation.